Available online at www.sciencedirect.com
ScienceDirect
Progress in Natural Science 18 (2008) 547–554
Progress in Natural Science
www.elsevier.com/locate/pnsc

Evaluation of a 3dVAR system for the South China Sea

Xianjun Xiao [a,b,*], Dongxiao Wang [a], Changxiang Yan [c], Jiang Zhu [c]

[a] *LED, South China Sea Institute of Oceanology, Chinese Academy of Sciences, Guangzhou 510301, China*
[b] *NCC, China Meteorological Administration, Beijing 100081, China*
[c] *Institute of Atmospheric Physics, Chinese Academy of Sciences, Beijing 100029, China*

Received 25 July 2007; received in revised form 10 December 2007; accepted 12 December 2007

Abstract

The authors evaluate a three-dimensional variational (3dVAR) system for the South China Sea (SCS) in this study. The assimilation method applied in the system takes into consideration error correlation along each ground track and uses recursive filter for optimization. Data from three R/V cruises during the spring and summer of 1998 and the summer of 2000 are used to evaluate the system. The root-mean-square error and bias are reduced significantly and when the altimeter data are assimilated, the distribution of the error is much closer to the Gaussian distribution. Precipitation and river discharge in the southwestern SCS are reproduced, and the variability of sea surface height is efficiently transferred to the subsurface. The 3dVAR system performs well for each of the three cruises, suggesting that it is steady for routine usage.

Keywords: South China Sea; Three-dimensional variational data assimilation; Recursive filter

1. Introduction

The South China Sea (SCS) is the largest marginal sea in Southeast Asia, and has complicated topography. It is connected with both Pacific and Indian Oceans by several straits. The SCS circulation has distinct seasonal variability due to the monsoon forcing. However, there is a large uncertainty in modeling the SCS circulation, because the forcing fields are inaccurate and the model parameters are not well known. Data assimilation can improve the SCS simulation.

At present, there are two categories of methods for assimilating altimeter data: the statistical method and the dynamic method. The statistical method [1–4] projects sea surface conditions to the subsurface using the statistical relationship between the altimeter data and the variables at the subsurface. It can be implemented easily but the result relies strongly on the statistical relationship and the statistical technique. The dynamic method [5–7], such as the one developed by Cooper [6], corrects the sea level and at the same time conserves the potential vorticity, and so the velocity changes as the potential vorticity redistributes vertically. This method is more complicated than the statistical one, but the variables are dynamically more consistent after the assimilation due to the dynamic constraints. We use the dynamic method mentioned above in this study.

Wang et al. [8] carried out blending assimilation experiments with TOPEX/Poseidon altimeter data. Although the large-scale features of the SCS circulation were effectively corrected, they did not correct the vertical structures because the altimeter data were not projected downward. Wu et al. [9] assimilated the TOPEX/Poseidon altimeter data in a three-dimensional primitive equation ocean model using the method of Cooper et al. [6], and improved

* Corresponding author. Tel.: +86 10 68408035; fax: +86 10 68408508.
E-mail address: xiaoxj@cma.gov.cn (X. Xiao).

1002-0071/$ - see front matter © 2007 National Natural Science Foundation of China and Chinese Academy of Sciences. Published by Elsevier Limited and Science in China Press. All rights reserved.
doi:10.1016/j.pnsc.2007.12.007

the large-scale features of the SCS circulation. They also analyzed interannual variability of the SCS circulation based on their assimilation [10].

The scarcity of observational data in the SCS makes it difficult to assess these data assimilations, so studies tend to focus on the large-scale features that can be easily evaluated. So far, there is no comprehensive assessment of the data assimilation using altimeter data by other observational data. Chu et al. [11] evaluated the US Navy's Modular Ocean Data Assimilation System (MODAS) using the data from the SCS monsoon experiment (SCSMEX) in 1998. However, 1998 is a warm-event year for the SCS [12], with typical distributions of temperature and salinity.

It is a challenge to reproduce the SCS circulation, because simple data assimilation systems (such as nudging or blending) are not good enough. Here, we present a three-dimensional variational (3dVAR) assimilation system of the SCS, and evaluate its performance using *in situ* data from three R/V cruises. Since current measurements are very limited, we can only assess the temperature and salinity of the 3dVAR system with CTD data from three cruises in spring and summer of 1998 and summer of 2000.

2. Model and data

The model used for the data assimilation is the Princeton ocean model (POM), which uses primitive equations and free surface. Its sigma coordinate allows the vertical resolution to vary over the water column, which can be as shallow as 5 m and as deep as 5500 m. There are 23 vertical layers. The number of the grid boxes is 100 by 60; they are distributed inhomogeneously over the model domain, with an average horizontal resolution of 35 km and the finest of 17 km. The model grid and topography are shown in Fig. 1(a).

The model was initialized by the climatological temperature and salinity from the World Ocean Atlas 2001 dataset (WOA01) [13] and forced by climatological monthly winds of ERA-40 reanalysis [14], starting in January. After three years of spin-up from a state of rest, the upper ocean approached an equilibrium state. Then, the model was forced by daily sea-surface winds from ERA-40 on the 1st of January, 1998. The surface heat fluxes were from the "NCEP/NCAR reanalysis 1" [15], which include monthly mean sensible and latent heat fluxes, long-wave and short-wave radiation fluxes. The lateral open boundary conditions for temperature, salinity, current, and sea surface height were from "ECCO-SIO 0" [16].

The observational data assimilated into the model are the sea surface anomaly from altimeter data (altimeter ocean pathfinder TOPEX/Poseidon 9.2). The along-track resolution of the TOPEX/Poseidon data is 6 km. A 5-point running mean was applied three times before the smoothed data were interpolated onto an 80-km interval used in the assimilation. These data manipulations are necessary to ensure the convergence of the large matrix used in the assimilation procedure.

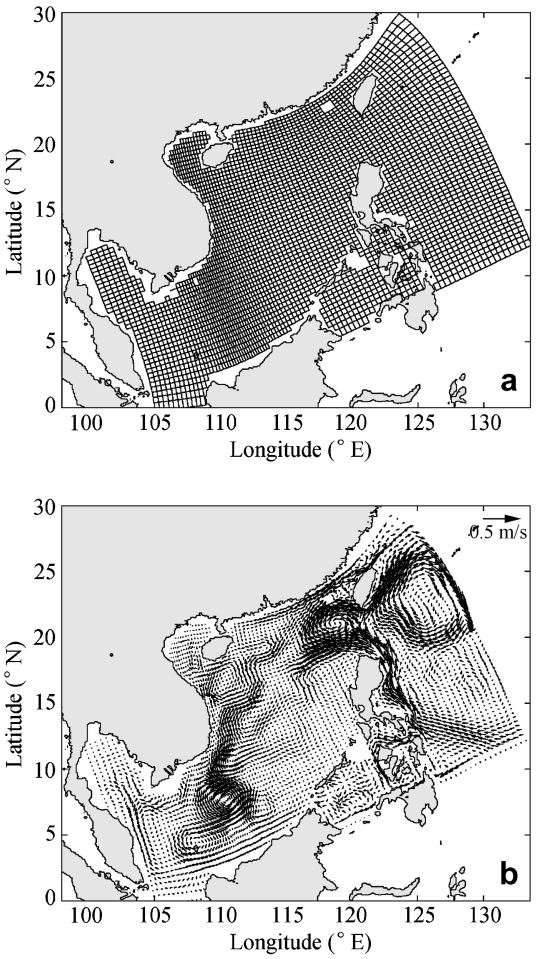

Fig. 1. The grid of the model and the simulated currents. (a) The SCS model basin and grid (the grid distribution is inhomogeneous and the grid along the west boundary of Vietnam in the south of SCS is finest); (b) the simulated monthly mean currents at 30 m in August of 1998.

3. Assimilation scheme

The 3dVAR system used in this study was originally developed by Zhu and Yan [17–19]. The control variables are temperature and salinity. There are two steps involved. During the first step, the control variables are retrieved from the altimeter data along each ground track. The optimum interpolation is then applied to the control variables obtained during the first step at each vertical level, to produce the final analysis of the control variables. Here, we will only describe the two improvements for the SCS 3dVAR model. First, when retrieving T–S (temperature–salinity) scatter diagram, the assimilation is done along each ground track of the satellite. Second, the recursive filter [20] is used for preconditioning, which avoids the inverse calculation of the background error covariance matrix explicitly.

The original method of Zhu and Yan assimilates altimeter data at individual locations, which does not account for the correlation of error between tracks. As a result, the T–S diagrams at different points were not correlated,

and the control variables were only optimized in one dimension. The error of T–S diagram at a single point was minimized only for that location, but it may not give the minimum for the whole assimilation region. To account for error correlation along a ground track, the one-dimensional T/S array in the vertical direction has been replaced by the two-dimensional one in both vertical and horizontal directions in the new 3dVAR system.

The second improvement is to speed up the computation. The dimension of background error covariance matrix is the square of the number of model grid points. A huge amount of computering resource is required to directly calculate the inverse of the covariance matrix. Therefore, we introduced the recursive filter [20] in the new system.

First, we define the new analytical variables of temperature and salinity as W_T, W_S, F_T, and F_S to be the recursive filter operators of T and S, respectively, where T and S are the analytical variables of temperature and salinity. The background temperature and salinity are denoted by T_b and S_b. Let

$$F_T W_T = T - T_\mathrm{b}, \quad F_S W_S = S - S_\mathrm{b} \tag{1}$$

According to the definition of recursive filter, the background error covariance E_T and E_S of temperature and salinity can be represented as

$$E_T = F_T F_T^\mathrm{T}, \quad E_S = F_S F_S^\mathrm{T} \tag{2}$$

The original cost function J of Zhu and Yan [17–19] is

$$J = \frac{1}{2}(T - T_\mathrm{b})^\mathrm{T} E_T^{-1}(T - T_\mathrm{b}) + \frac{1}{2}(S - G(T))^\mathrm{T} E_S^{-1}(S - G(T)) + \frac{1}{2\sigma^2}(h(T,S) - h_\mathrm{m} - h_0)^2 \tag{3}$$

Here, the function $G(T)$ is the nonlinear relationship between T and S calculated from the WOA01 [13], the mean sea surface height h_m is the statistic of model result, the observational sea surface height coming from altimeter data is denoted by h_0, the observational error variance σ is set to be 0.0002, and the steric height

$$h(T,S) = -\int_0^{z_\mathrm{m}} \frac{\rho(T,S,p) - \rho_0(p)}{\rho_0(p)}\,\mathrm{d}z \tag{4}$$

We treat h as the equivalent of the ocean dynamic topography. The density of sea water is $\rho(T,S,p)$, and its reference density is $\rho_0(p) = \rho(0,35,p)$. The reference depth z_m for the SCS is 1000 m. Using Eqs. (1) and (2), Eq. (3) gives the new cost function:

$$J = \frac{1}{2}W_T^\mathrm{T} W_T + \frac{1}{2}W_S^\mathrm{T} W_S + \frac{1}{2\sigma^2}(h(T_\mathrm{b} + F_T W_T, S_\mathrm{b} + F_S W_S) - h_\mathrm{m} - h_0)^2 \tag{5}$$

The de-correlation scales of T (S) are 450 and 650 km (420 and 510 km) in the latitudinal and longitudinal directions, respectively, for the background error covariance matrix. The variances of T and S are 4 °C and 0.2 psu, respectively.

4. Results

Fig. 1(b) shows the monthly mean current fields at 30 m depth in August 1998 derived from the 3dVAR system. We can see that the 3dVAR system can reproduce the SCS general circulation reasonably well. The Kuroshio intrudes the SCS through the Luzon strait as a loop current in the north of SCS. The strong west boundary current along Vietnam flew into the south of SCS. And the off shore jet of Vietnam originated from the west boundary current. Some mesoscale eddy scattered in SCS can also be seen in Fig. 1(b).

Next, we will evaluate the system based on the T–S scatter diagram, sections of temperature and salinity distributions, and the statistics of errors. The observational data used for this evaluation are the multi-cruise hydrographic data, including SCSMEX in 1998 and a summer cruise in 2000. The observational periods are from April 22 to May 26 for the 1998 spring cruise with 592 stations of CTDs (Fig. 2(a)), from June 4 to July 21 for the 1998 summer cruise with 712 stations of CTDs (Fig. 2(b)), and from August 9 to September 3 of 2000 with 89 stations of CTDs (Fig. 2(c)).

4.1. T–S diagram

Fig. 3 shows the T–S diagrams from the CTD data, model simulations, and data assimilations. The surface, subsurface, intermediate, and deep waters in the SCS were identified by both simulations and assimilations. However, the difference between intermediate and deep waters was not clear in the simulations and assimilations. This inability to separate the intermediate water from the deep water is common to ocean models, which results from the excessive mixing in the vertical direction. There is sufficient evidence in the observations that the surface and subsurface water in the western Pacific intrudes the SCS [21]. This intrusion in the simulation and assimilation was much stronger than that suggested by the observation, likely caused by too strong constraint on the improper dynamics of the model. Therefore, improvement in the vicinity of the Luzon Strait was not significant. The assimilation slightly improved the high-salinity water in the surface in the simulation (Fig. 3, upper panels).

The T–S diagram in the summer of 1998 (Fig. 3, middle panel) was different from that in the spring. The difference between the intermediate and deep waters was more evident in the two models as compared with that in the spring of 1998. In the assimilation, however, the salinity of the surface and subsurface waters was little lower. The cause of this degrading needs further study.

There should be more low-salinity water after the onset of the summer monsoon due to precipitation. The salinity of surface and subsurface waters in the simulation for the summer of 2000, however, was abnormally higher than that in the reality (Fig. 3, lower panels). With data assimilation, this model error was corrected.

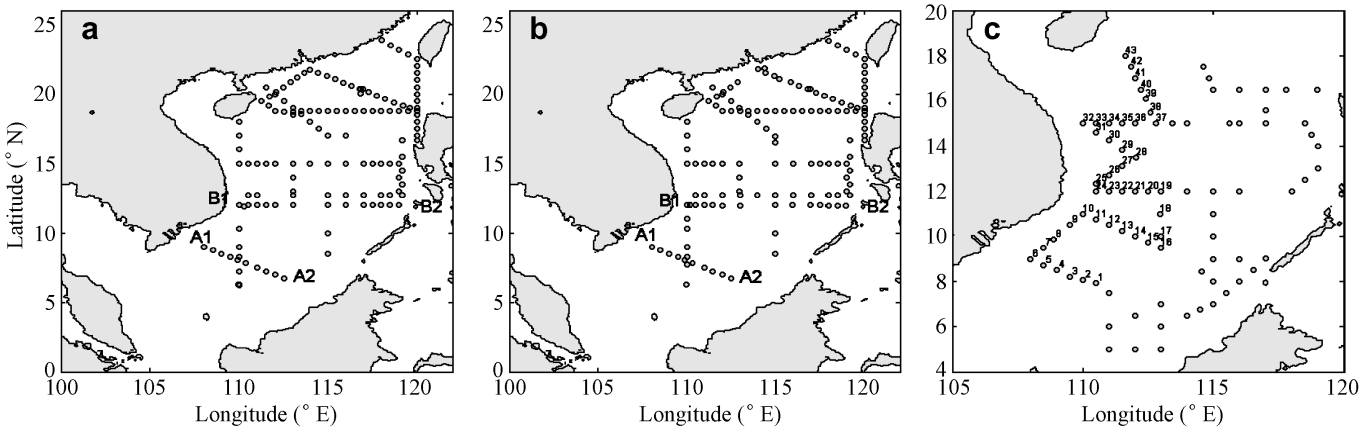

Fig. 2. Stations of *in situ* data taken from three cruises during (a) spring of 1998, (b) summer of 1998, and (c) summer of 2000.

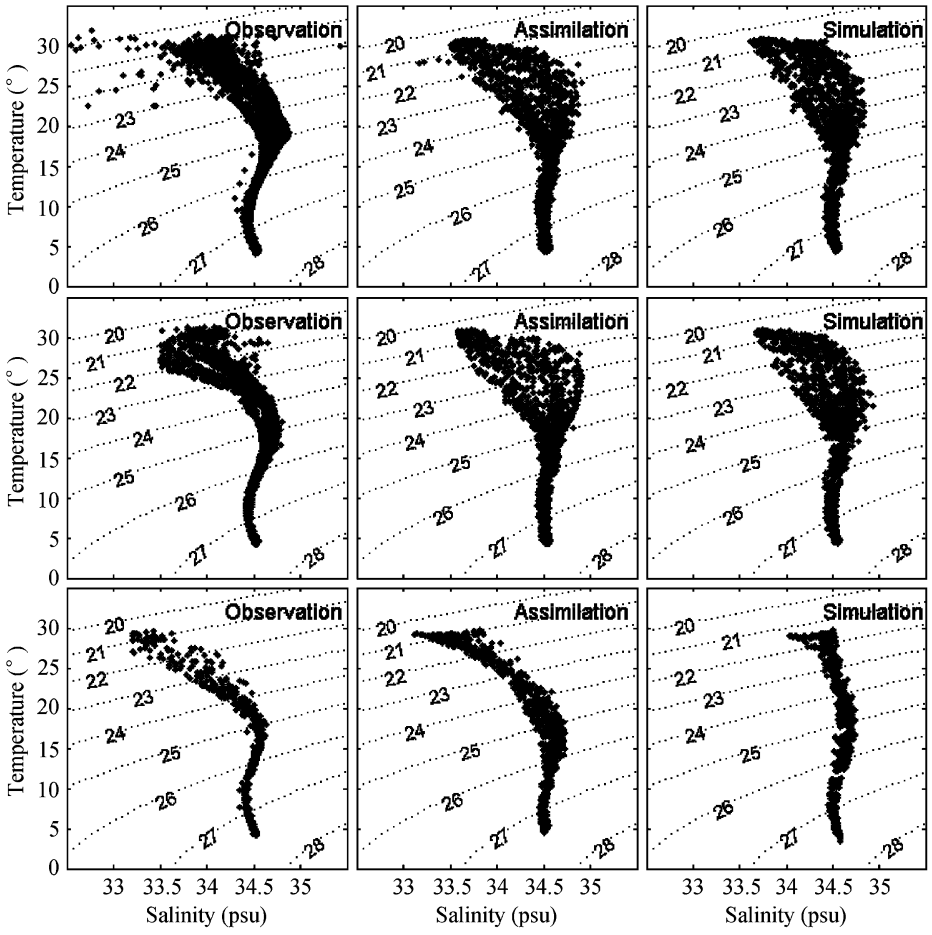

Fig. 3. Scatter diagrams of temperature and salinity. The left, middle, and right panels are observations, assimilations, and simulations, respectively. The top, middle, and bottom panels are spring of 1998, summer of 1998, and summer of 2000, respectively. The dotted line represents the potential density.

4.2. Error statistics

Here, we analyze the errors of both assimilation and simulation in three ways. First, the mean bias of error at each level will be analyzed to show the error distribution in the vertical direction. Then, the root-mean-square error (RMSE) at each level will be compared. Finally, the total standard deviation of error with the probability distribution of error will be calculated.

The assimilation biases of temperature were larger than the simulated one from the sea surface to the depth of 100 m, and the mean bias of assimilation was less than 1 °C in terms of the hydrography for each cruise. The assimilation successfully corrected the model bias below

100 m for each cruise (Fig. 4). The temperature of assimilation was 0–1 °C higher than observations between 100 and 200 m depths, and 0.5 °C lower than observations or less below 200 m. The improvement of temperature from 200 m depth downward in the summer of 2000 was most obvious, and the assimilation bias was reduced from 0 to 0.15 °C.

The assimilation also improved salinity (Fig. 4), especially for the summer of 2000. The bias of error above 100 m depth was between −0.1 and 0.15 psu, and larger than the bias below 100 m, which was between −0.05 and 0.05 psu. The model error without the assimilation was above 100 m for the summer of 2000, with a bias between 0.4 and 1.4 °C. The bias was reduced from 0.2 to 0.4 °C with the assimilation. The improvement was not obvious during these periods of assessments.

Between the depth of 200 and 500 m, the RMSEs of the assimilations, ranging from 0.3 to 1.5, are much smaller than those without the assimilation (Fig. 4). There was little improvement above 100 m; the RMSEs of the assimilations are between 0.5 and 3.5 in the average, even worse for the summer of 2000. The possible reason is that the upper ocean is modulated by the heat flux from the atmosphere, and so the result may be affected strongly by the improperly parameterized mixing process and the restoring of heat flux.

The RMSEs of salinity are improved a little (Fig. 4). The error is between 0.1 and 0.4, slightly higher above 100 m. We suspect that the lack of freshwater flux cause the error, because the SCS is situated in the area of prevailing monsoons, and evaporation and precipitation are vital to the salinity in the upper 100 m. The RMSEs are between 0.02 and 0.10 below 100 m.

Temperature and salinity from the assimilation are closer to the typically normal distribution (Fig. 5). In other words, the distribution of error associated with the assimilations is more reasonable. The standard deviation of temperature in the assimilation is 1.5 °C, which is smaller than that of the simulation. For the summer of 2000, the deviation of temperature in the assimilation is slightly bigger than that of the simulation, but they are both small, 1.4 and 1.1 °C, respectively. The standard deviation of salinity is reduced by about 0.04 psu, compared with the simulation value of 0.24 psu or so.

4.3. Stratification

Two vertical temperature/salinity sections are analyzed for the cruises. Several vertical sections in a sequential observational period are analyzed jointly because the duration of 2000 cruise is much longer.

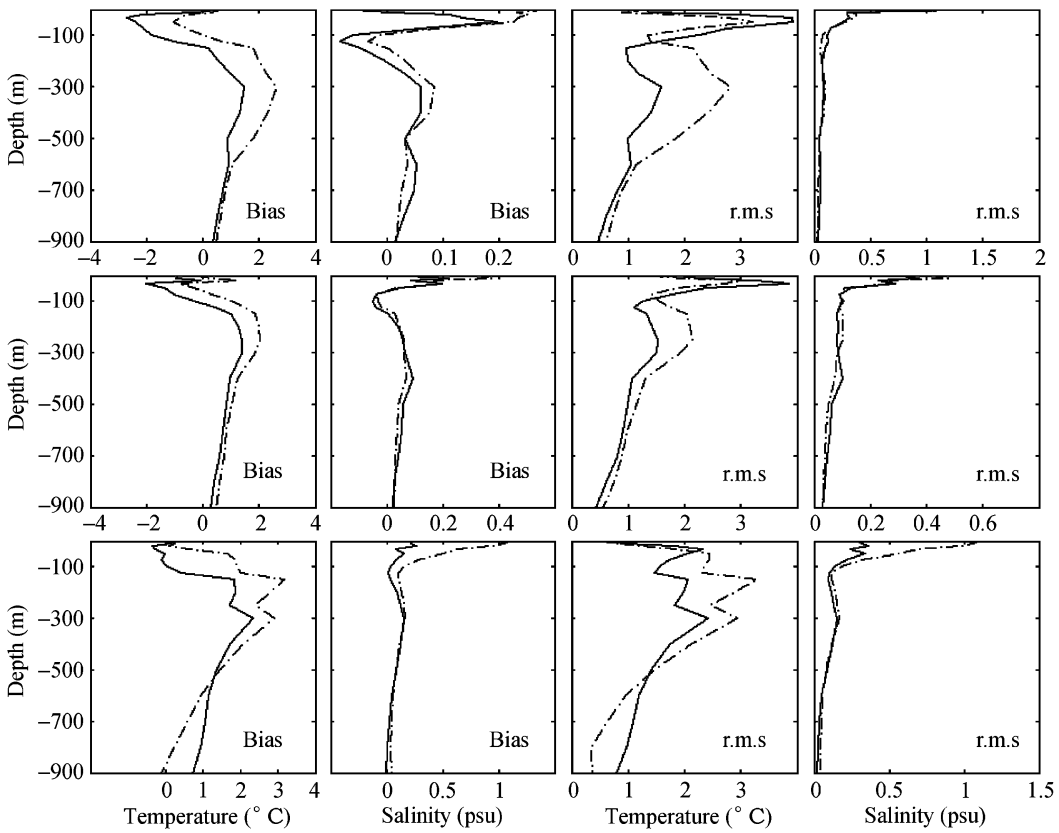

Fig. 4. The error statistics about temperature and salinity in vertical profiles. The solid line is the result of assimilation and the dashed line is of the simulation. The first column is the bias of temperature, the second for salinity. The bias is the mean at each level that assimilation subtract observation. The third column is the r.m.s. error of temperature and the last column is the salinity. The top panel is the result of spring cruise in 1998, the middle for summer cruise in 1998, and the bottom for summer cruise in 2000.

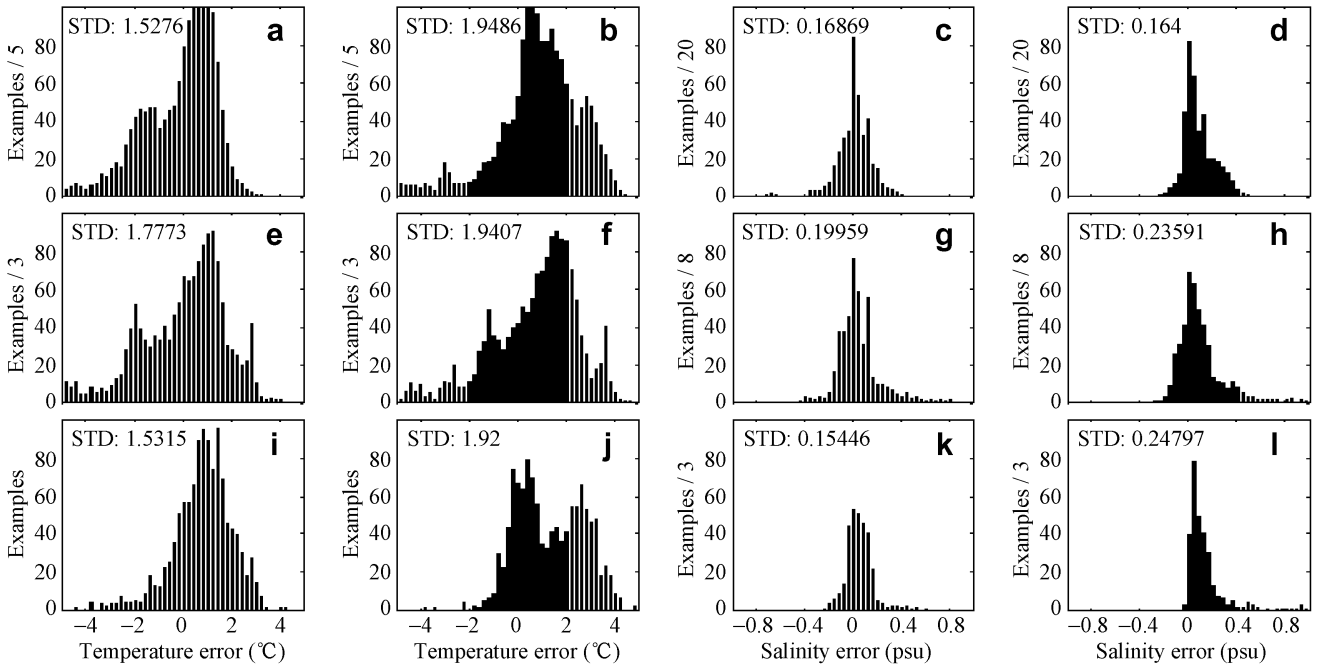

Fig. 5. Distribution of temperature and salinity error. The *x*-axis represents error (assimilation subtract observation or simulation subtract observation), and the *y*-axis represents the number of samples. The *y*-axis of (a), (b) is scaled by 5, of (c), (d) scaled by 20, of (e), (f), (k), (l) scaled by 3, and of (g), (h) scaled by 8. (a–d) Result of spring cruise in 1998, (e–h) for summer cruise in 1998, and (i–l) for summer cruise in 2000. The first and the second column are the temperature error of assimilation and simulation, respectively. The third and the fourth column are the salinity error of assimilation and simulation, respectively. The superimposed STD denotes total standard deviations of error. The unit of STD for temperature is °C and for salinity is psu.

Assimilation improved the temperature somewhat. The isotherm rose up and the grade of thermocline was increased after the assimilation for the section A1A2 of spring 1998 (Fig. 6). As a result, the seasonal thermocline is more evident. The mixed layer is still shallower and the subsurface temperature is lower. All these can be attributed to the weak mixing in the upper layer. The error statistics described in Section 4.2 also showed that the error above 100 m was bigger than that at the intermediate depth. This error may come from the poor quality of heat fluxes in the region. The heat fluxes could determine the thermal structure in the upper layer [22] to a large extent, and so improvement of result solely by assimilation may be difficult. The situations along other sections are similar (not shown).

The salinity is improved mostly in the upper layer by the assimilation, and the freshwater cover in the SCS is modeled. Since the SCS is located in the area of prevailing monsoons, the abundant precipitation in summer could reduce sea surface salinity (SSS), which results in a barrier layer. A barrier layer could impact the local circulation, in particular, the vertical diffusion of heat. All the information about the precipitation contained in the sea-level anomaly is reflected in the SSS. Because of the constraint of the nonlinear relationship between temperature and salinity, the improvement is more obvious. The 50 m salinity of section A1A2 in spring (Fig. 6) and summer (not shown) of 1998 are both about 34 psu in the assimilation. The results are 0.2 psu lower than that without the assimilation, and close to the observations of 33.9 and 34 psu, respectively. The freshwater covers are found both in the vertical section B1B2 in spring (Fig. 6) and summer (not shown) of 1998. The difference between them is the position. The freshwater cover in the assimilation is located between 113°E and 115°E, which is closer to the position of the observation compared with the simulation, whose freshwater cover is located in 116.5°E. We also analyzed the consecutive cruise section off the southeast coast of Vietnam extending in the summer of 2000. There existed large freshwater cover from the Mekong runoff in the observation. This feature is evident in the assimilation, but not in the simulation (Fig. 6). Because the vertical section was local, the SSS of assimilation and simulation in the summer of 1998 was compared (not shown). The difference of SSS between the assimilation and simulation was small in the northern and central SCS, but distinct on the shelf of the northern SCS, the coast of Vietnam, and the southeastern SCS. In the assimilation, there are two obvious low-salinity areas. One is the low-salinity tongue from the Mekong runoff extending from 10°N to north in the southeast coast of Vietnam, which is expressed as the northern extension of the 33.6 psu isoline. The other one, resulted from strong precipitation, is a low-salinity band extending to 10°N, whose centre is off the coast of the southeastern SCS (3°N, 112°E). The vertical section A1A2 is in the Sunda shelf of the SCS stretching from the south of the Indochina Peninsula to the edge of the warm pool located in the southeastern SCS. The northern part of the vertical section is affected by the low-salinity tongue and the southern part of it is near the low-salinity band in warm pool area. So the

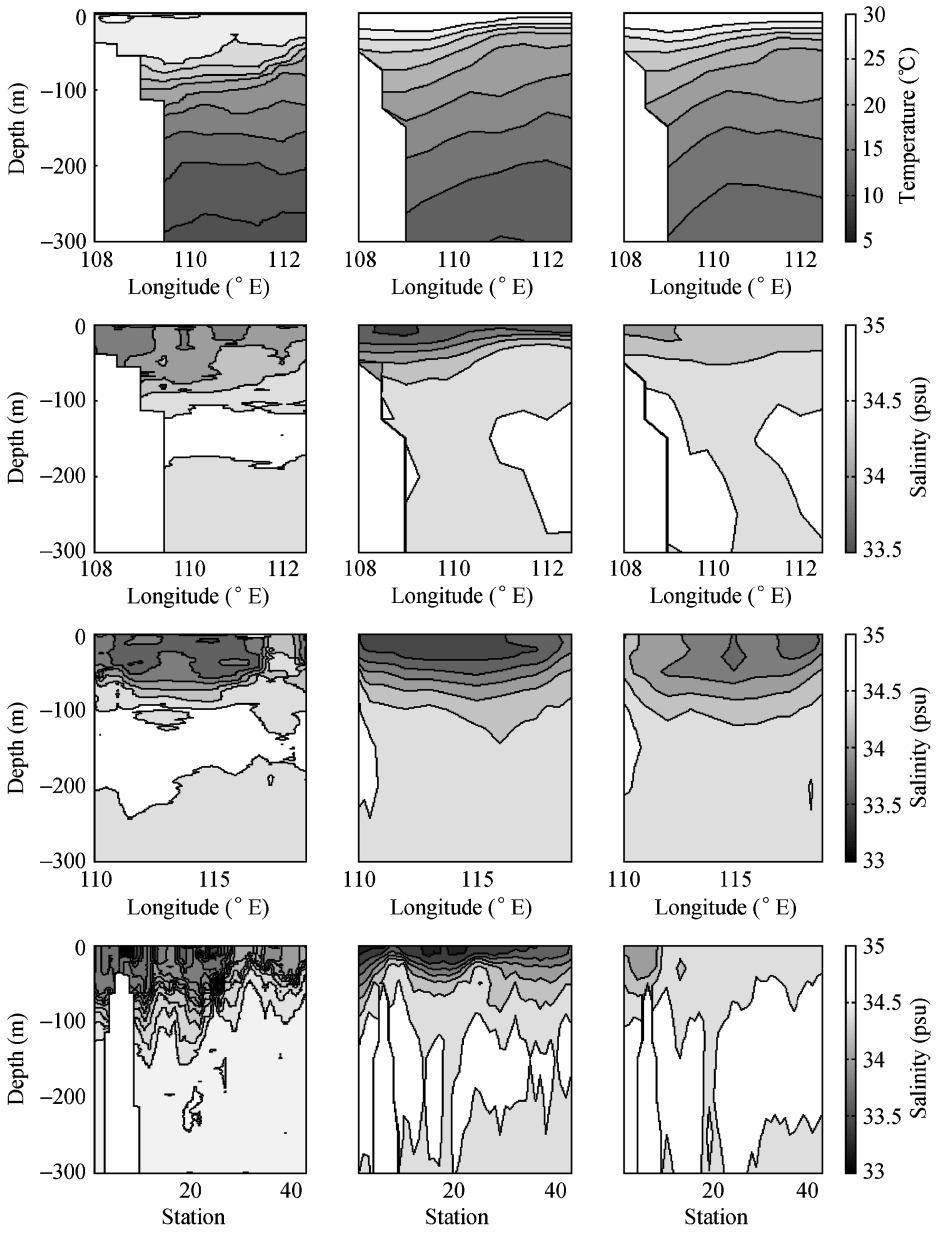

Fig. 6. Vertical sections of temperature and salinity. The top two panels show the temperature and salinity of section A1A2 in Fig. 2(a) (spring of 1998), respectively; the third panel shows the salinity of section B1B2 in Fig. 2(a); the bottom panel shows the salinity of the consecutive section in Fig. 2(c) (summer of 2000), following the ascending order of the number. The unit of salinity is psu, and of temperature is °C.

upper layer of the vertical section shows a low salinity. The vertical section B1B2 is near 12°N across the southern SCS from west to east. The west end of the section is close to the low-salinity tongue of Mekong runoff, so the low-salinity core is in the western part. This feature is reproduced by the assimilation but not in the simulation. In summary, freshwater covers, which are either too weak or absent in the simulation, are reproduced well by the assimilation.

4.4. Robustness of the 3dVAR system

Since the SCS is abnormally warm in 1998 [12], the characteristics of its temperature, salinity and circulation are different from that of 2000, a normal year. However, the 3dVAR system works, as we have seen above, for a warm year or a normal year.

The structures of the assimilated temperature and salinity are different in different years. The *T*–*S* diagrams show that the assimilations increase the salinity at both surface and subsurface in 1998 and reduce the SSS in 2000, and that influence of assimilation is not a systematic error and could reproduce the interannual variability more reasonably than the simulation. The influence of assimilation for different cruises is different according to the statistic analysis of each vertical level. Below 200 m the temperature bias is reduced more in 2000 than in 1998. There are posi-

tive or negative biases in the salinity of the upper layer in 1998, but are mostly positive in 2000. The bias or RMSE is smaller in summer than that in spring. The salinity error in the upper layer in the summer cruise of 2000 is smaller than that in the other two cruises. The distribution of error is uniform with a large standard deviation in 1998. It was close to the distribution of Gaussian with a smaller standard deviation in 2000 (Fig. 5). The number of samples in the temperature–salinity section is limited and therefore not compared here.

The assimilation has improved the model simulation in different seasons and different years, and so we can conclude that the 3dVAR system is stable.

5. Conclusions

A 3dVAR system for the SCS is evaluated by multi-cruise data. Compared with the MODAS [11] assimilating multiple observational datasets including XBT and altimeter data among others, this 3dVAR system has only assimilated the altimeter data. The assimilation passes the ocean-state information hidden in the sea-level data into subsurface ocean. The results are promising, which could improve the simulation in a normal year (2000) as well as in an abnormally warm year (1998). Particularly, the assimilation is able to reproduce the freshwater covers. This is an important feature of the SCS, resulted from both the river runoff and precipitation. Recently, we have implemented the 3dVAR system to the 10-year reanalysis of the SCS, which will be reported in a separate paper.

Acknowledgements

This work was supported by the National Natural Science Foundation of China (Grant Nos. 40476013 and 40625017) and MOST of China (Grant Nos. 2006AA09Z156 and 2002AA639250). The ECCO-SIO 0 data were provided by the Consortium for Estimating the Circulation and Climate of the Ocean (ECCO) funded by the National Oceanographic Partnership Program. NCEP Reanalysis data were provided by the NOAA/OAR/ESRL PSD, Boulder, Colorado, USA, from their Web site at http://www.cdc.noaa.gov.

References

[1] DeMey P, Robinson A. Assimilation of altimeter eddy fields in a limited-area quasi-geostrophic model. J Phys Oceanogr 1987;17:2280–93.

[2] Holland WR, Malanotte-Rizzoli P. Assimilation of altimeter data into an ocean circulation model: space versus time resolution studies. J Phys Oceanogr 1989;19:1507–34.

[3] Mellor GL, Ezer T. A Gulf Stream model and an altimetry assimilation scheme. J Geophys Res 1991;96(C5):8779–95.

[4] Ezer T, Mellor GL. Continuous assimilation of GEOSAT altimeter data into a three-dimensional primitive equation Gulf Stream model. J Phys Oceanogr 1994;24(4):832–47.

[5] Haines K. A direct method for assimilating sea surface height data into ocean models with adjustments to the deep circulation. J Phys Oceanogr 1991;21:843–68.

[6] Cooper M, Haines K. Data assimilation with water property conservation. J Geophys Res 1996;101:1059–77.

[7] Drakopoulos PG, Haines K, Wu P. Altimetric assimilation in a Mediterranean general circulation model. J Geophys Res 1997;102:10509–23.

[8] Wang D, Shi P, Yang K, et al. Assimilation experiment of blending TOPEX altimeter data in the South China Sea. Oceanol Limnol Sin 2001;32(1):101–7, [in Chinese].

[9] Wu CR, Shaw PT. Assimilation altimetric data into a South China Sea Model. J Geophys Res 1999;104(C12):29987–30005.

[10] Wu CR, Chang CWJ. Interannual variability of the South China Sea in a data assimilation model. Geophys Res Lett 2005;32(17):L17611. doi:10.1029/2005GL023798.

[11] Chu PC, Wang GH, Fan CW. Evaluation of the U.S. Navy's Modular Ocean Data Assimilation System (MODAS) using the South China Sea Monsoon Experiment (SCSMEX) data. J Oceanogr 2004;60:1007–21.

[12] Wang D, Xie Q, Du Y, et al. The 1997–1998 warm event in the South China Sea. Chin Sci Bull 2002;47(14):1221–7.

[13] Conkright ME, Locarnini RA, Garcia HE, et al. World ocean Atlas 2001: objective analyses, data statistics, and figures. Available from: http://www.nodc.noaa.gov/General/NODCPubs/ [accessed 06-12-2006].

[14] Uppala SM, Kållberg PW, Simmons AJ, et al. The ERA-40 reanalysis. Q J R Meteorol Soc 2005;131:2961–3012.

[15] Kalnay E, Kanamitsu M, Kistler R, et al. The NCEP/NCAR 40-year reanalysis project. Bull Amer Meteor Soc 1996;77:437–70.

[16] The ECCO Consortium: Stammer D, et al. The consortium for estimating the circulation and climate of the ocean (ECCO). http://www.ecco-group.org/report_series.htm [accessed 06-12-2006].

[17] Yan C, Zhu J, Li R, et al. Roles of vertical correlations of background error and *T–S* relations in estimation of temperature and salinity profiles from sea surface dynamic height. J Geophys Res 2004;109:c08010. doi:10.1029/2003JC002224.

[18] Zhu J, Yan C. Nonlinear balance constraints in 3DVAR data assimilation. Sci China (Ser D) 2006;49:331–6.

[19] Zhu J, Zhou GQ, Yan C, et al. A three-dimensional variational ocean data assimilation system: scheme and preliminary results. Sci China (Ser D) 2006;49(12):1212–22.

[20] Purser RJ, Wu WS, Parrish DF, et al. Numerical aspects of the application of recursive filters to variational statistical analysis. Part I: Spatially homogeneous and isotropic Gaussian covariances. Mon Wea Rev 2003;131:1524–35.

[21] Wang F, Zhao Y, Feng Z. Thermohaline structure and variation of the South China Sea in the spring and summer of 1998. Acta Oceanol Sin 2001;23(05):1–13, [in Chinese].

[22] Liu Q, Wang D, Jia Y, et al. Seasonal variation and formation mechanism of the South China Sea warm water. Acta Oceanol Sin 2002;21(3):331–43.